

Slurry Erosion Behavior of Destabilized and Deep Cryogenically Treated Cr-Mn-Cu White Cast Irons

S. Gupta^a, A. Khandelwal^a, A.K. Ghose^a, I. Chakrabarty^a

^a Department of Metallurgical Engineering, Indian Institute of Technology (Banaras Hindu University), Varanasi 221005, India.

Keywords:

Alloy white cast iron
Castings
Optical microscopy
Erosive wear
Corrosion
Cryogenic treatment

ABSTRACT

The effects of destabilization treatment and destabilization followed by cryogenic treatment have been evaluated on the microstructural evolution and sand-water slurry erosion behavior of Cr-Mn-Cu white cast irons. The phase transformations after the destabilization and cryotreatment have been characterized by bulk hardness measurement, optical and scanning electron microscopy, x-ray diffraction analysis. The static corrosion rate has been measured in tap water (with pH=7) and the erosion-corrosion behavior has been studied by slurry pot tester using sand-water slurry. The test results indicate that the cryogenic treatment has a significant effect in minimizing the as-cast retained austenite content and transforming into martensitic and bainitic matrix embedded with ultra-fine M7C3 alloy carbides. In contrast, by conventional destabilization treatment retained austenite in the matrix are not fully eliminated. The slurry erosive wear resistance has been compared with reference to destabilized and cryotreated high chromium iron samples which are commonly employed for such applications. The cryotreated Cr-Mn-Cu irons have exhibited a comparable erosive wear performance to those of high chromium irons. Higher hardness combined with improved corrosion resistance result in better slurry erosion resistance.

Corresponding author:

I. Chakrabarty
Department of Metallurgical
Engineering, Indian Institute of
Technology (Banaras Hindu
University), Varanasi 221005 India.
E-mail: ichakraborty.met@itbhu.ac.in

© 2016 Published by Faculty of Engineering

1. INTRODUCTION

A combined action of electrochemical corrosion and mechanical damage due to erosion by the solid particles suspended in a liquid slurry medium accelerates failure to many critical components. The effect of this combined action is synergistic in nature that is corrosion accelerates wear and vice-versa. Thin passivating surface layers that protect the

material from corrosion are worn out by the impinging eroding particles in the slurry and further corrosion increases. Plastic deformation of the metal surface during wear can also generate localized high energy sites more prone to corrosion than the unworn sites. High chromium and nickel-chromium white cast irons are potent materials for corrosion-erosion applications such as in the mining, earth moving, cement and coal industries [1-4]. The carbide

morphology and the matrix phase are the two influencing factors contributing to maximum wear resistance, toughness and corrosion. Discontinuous plate like eutectic M7C3 carbides along with tough matrix embedded with fine secondary alloy carbides are preferable for such applications [5,7]. A thin passive layer is formed on the surface due to high percentage of chromium in the solid solution [8,9].

Beside the developments in the high chromium and nickel-chromium irons there has been continuing interest in the development of substitute alloy irons to provide either a partial or total replacement of costly and scarce alloying elements viz. Ni, Mo etc. A new class of chromium–manganese alloy irons has been developed with manganese, a cheaper alloying addition to produce a predominantly austenitic matrix in as-cast condition by suppressing pearlitic transformation [10-12]. Copper addition to chromium–manganese irons reported to be beneficial because of its partitioning tendency to austenite phase and it enhances resistance to aqueous corrosion [13-17].

The as-cast austenitic matrix is conventionally destabilized by a destabilization or destabilization treatment to transform as-cast austenite to martensitic and/or fine bainitic matrix embedded with fine secondary carbides [1,2]. But even after such conventional destabilization the retained austenite cannot be totally transformed. Cryogenic treatment is successfully employed especially in tool steels [18-32] and high chromium cast irons [33-37] to minimize the retained austenite content as far as possible. The consequent improvement in wear resistance has been attributed to i) transformation of retained austenite to martensite, ii) conditioning of martensite at low temperature and iii) enhanced volume percentage of refined secondary carbide precipitation. In a recent study, Shaohong Li et. al [31] have verified the mechanism of the refined carbide precipitation by internal friction method and transmission electron microscopy, in tool steels on deep cryogenic treatment. The high internal stress developed from austenite to martensite transformation is responsible for modification of carbide precipitation. The martensite lattice contraction causes to segregate interstitial carbon atoms at the nearly

moving dislocations. The tetragonality becomes very low as a consequence. A strong interaction in between the time dependent strain field of dislocation and the segregated carbon atoms is produced. The segregated carbon atoms form clusters at nearby dislocations forming nuclei for carbide precipitation during subsequent warming up to room temperature or tempering. These uniformly dispersed secondary carbides are responsible for the improvement of properties on deep cryogenic treatment.

The aim of the present article is to study the effect of destabilization and cryogenic treatment on the microstructural evolution and consequent erosive wear behavior of Cr-Mn-Cu white cast iron in sand-water slurry media.

2. EXPERIMENTAL PROCEDURE

The alloy irons were melted in a basic lined high frequency induction furnace. Cylindrical test bars and wear test samples were cast in sodium silicate –CO₂ bonded sand moulds with a pouring temperature of 1773K (1500 °C). For comparison of wear behaviour high chromium iron specimens were also cast; the chemical compositions analysed in ARL optical emission spectrometer are shown in Table 1.

Table 1. Chemical compositions of alloy irons cast.

Alloy irons	C%	Mn%	Si%	Cr%	Cu%
a)Cr-Mn-Cu iron	2.8	4.8	1.87	9.2	3.1
b) High Cr iron	2.9	0.53	0.32	16.3	-

Optimum destabilization temperature ranges and time for as-cast Cr-Mn-Cu irons were selected based on isochronal and isothermal heat treatments. Initially the as-cast samples were subjected to isochronal heat treatment for a fixed period of 1 hour in the temperature range of 973K (700 °C) to 1373K (1100 °C) in 373K (100 °C) steps and followed by air cooling to room temperature. In the optimum temperature range thus found from the isochronal treatment, the samples were isothermally treated for various soaking times and subsequently either air cooled or quenched in liquid nitrogen bath and kept immersed for 30 minutes for the cryogenic treatment. The wear samples were heat treated at the optimum temperature {1023K (750 °C)} and time (9 hours) obtained from isochronal and isothermal

treatments. High chromium irons were subjected to conventional destabilization at 1273K (1000 °C) for 9 hours and subsequently cryotreated. The microstructures of the alloy irons observed under optical and scanning electron microscopes. The bulk hardness at different heat treatment conditions were measured in Rockwell C- scale with 150 kgf load.

The retained austenite contents in a few selected samples were measured by x-ray diffraction analysis with Cu K α radiations. To avoid the effect of texture the samples were continuously rotated. The carbide volume percentages present in the alloys at different conditions were measured by electrolytic extraction of carbides. The carbide volume percentages thus determined were computed to estimate the retained austenite content in the matrix. A bath with 5 % concentrated HCl in ethyl alcohol was employed with sample as anode and a stainless steel plate as cathode for electrolytic extraction. The extraction was continued for about 20 hours with a current density of 5 mA/cm² and the extracted carbides were collected in a glycerine layer from the bottom of the bath. The volume percentages of the extracted carbides were calculated after drying at 343K (70 °C).

The static corrosion rate of the alloy irons was measured as per ASTM standard (ASTM G-1-72). Mirror polished rectangular specimens (10x10 mm.) were cleaned with water and acetone, dried and weighed in an electronic balance. The samples were suspended in a glass beaker with tap water (pH=7) for 168 hours at room temperature. After this period of immersion, the specimens were again cleaned thoroughly with water and acetone, dried and reweighed. The static corrosion rates were computed from the expression,

$$\text{Corrosion rate [in mg/decimeter}^2\text{/ day (mdd)]} = \frac{K.W}{(A.T.D)}$$

where, K= 2.4 x 106.D; W= weight loss in g nearest to 1 mg; A= surface area in square cm nearest to 0.01 cm²; T= duration in hours; D= density of the material in g/cc.

The erosive wear performance was evaluated in a slurry pot tester as shown in Fig. 1. Although the effect of impact angle of the slurry particle impingement cannot be evaluated by this set up, the relative wear performance in different heat

treatment conditions of the test alloy specimens can be well assessed with reference to the high chromium iron samples under identical conditions. Cylindrical wear specimens (10 mm. diameter x 50 mm. length) were ground with emery paper number 1000, cleaned with water and acetone, dried and fitted in the holding disc of the test rig. Specimens with similar heat treatment condition were placed at the

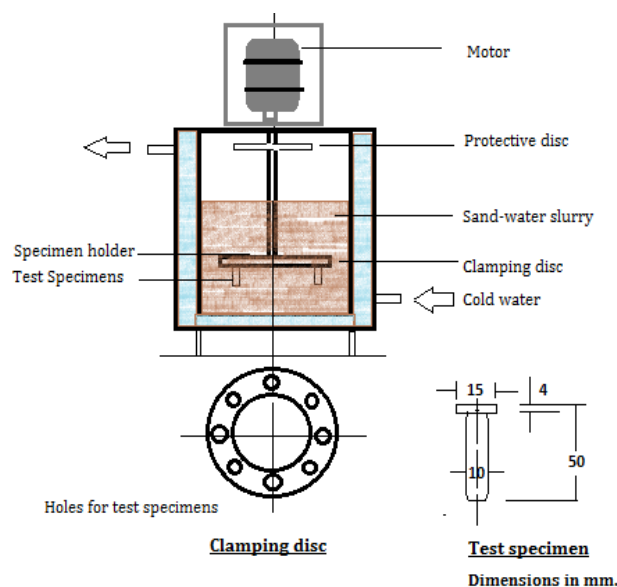


Fig. 1. Slurry erosion test set-up.

Two diametrical opposite position at the holding disc to avoid any biasness. The sand-water slurry was prepared with 60 % silica sand particles by weight in plain tap water. The details of the silica sand eroding particles are shown in Table 2.

Table 2. Details of silica sand used for slurry erosion test.

Erodent	Shape (Roundness) ^a	Average size, μm	Micro-hardness, Kg/mm ²
Silica sand	0.79	325	1100-1150

^a according to Rittenhouse sphericity scale

The specimens were rotated in the slurry for a total duration of 24 hours at 500 rpm which corresponds to a linear speed of 4.5 m/s. After every 6 hours of test run the specimens were taken out, cleaned, dried and the mass losses were noted. After 24 hours run the samples tips were cut off, cleaned ultrasonically in acetone and examined under scanning electron microscope for worn-out surface topography.

3. RESULTS AND DISCUSSION

3.1 Phase Transformation Behaviour

As revealed in the optical microstructure shown in Fig. 2, the as-cast Cr-Mn-Cu iron consists of predominantly austenitic matrix along with discontinuous eutectic carbides. The matrix structure is confirmed by XRD analysis, the austenite content has been estimated to be 87.63 % and the types of eutectic carbides are detected as M_7C_3 carbides (Fig. 3). The volume percent of these carbides has been estimated as 15.4 % from electrolytic extraction.

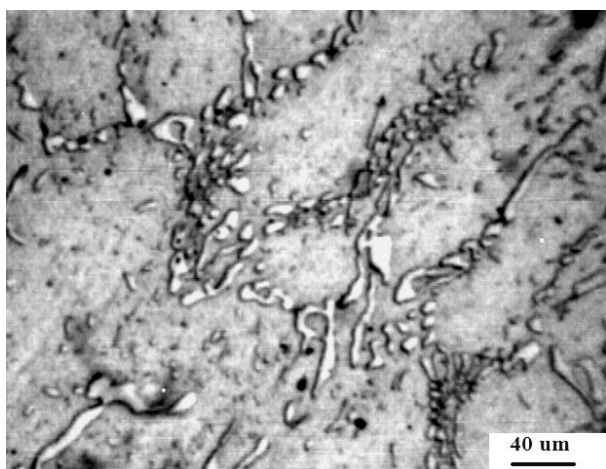


Fig. 2. Optical micrograph of as-cast Cr-Mn-Cu iron showing predominantly austenitic matrix.

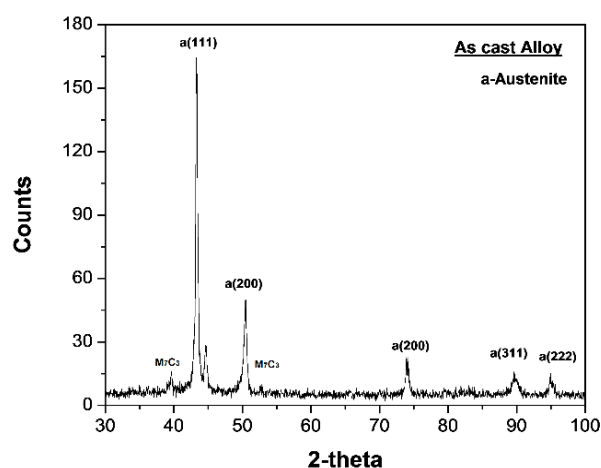


Fig. 3. XRD pattern of as-cast Cr-Mn-Cu alloy iron with Cu $K\alpha$ radiation.

The bulk hardness after isochronal treatment temperature attains a peak at a temperature around 1023K (750°C) and decreases with further increase in temperature. Fig. 4 shows the corresponding microstructural change in optical micrographs from which it can be inferred that

as the temperature is increased initially as-cast austenitic matrix is gradually transformed into martensitic and/or fine bainitic matrix along with fine alloy carbide precipitates.

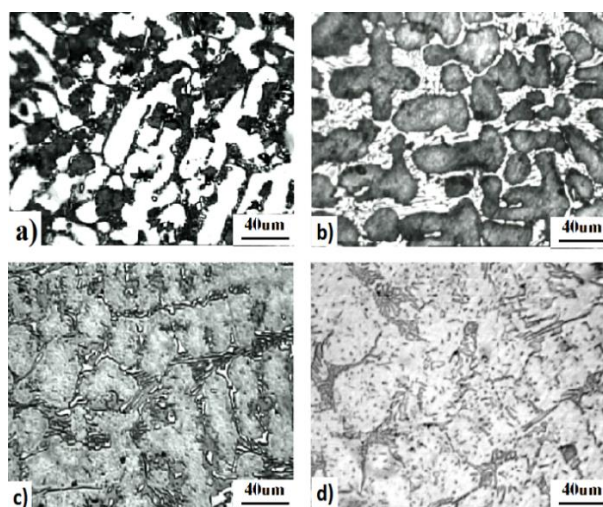


Fig. 4. Optical micrographs of isochronally treated alloy irons for 1 hour at a) 973K (700 °C), b) 1073K (800 °C), c) 1273K (1000 °C) and d) 1373K (1100 °C).

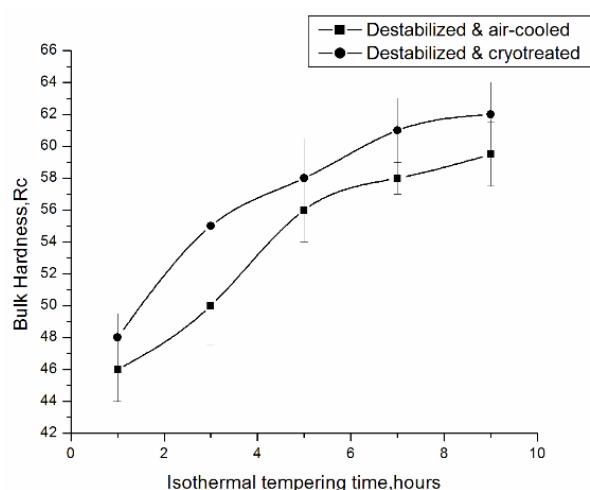


Fig. 5. Variation in bulk hardness with isothermal treatment time followed by a) cryotreatment and b) air cooling.

This results in an increase in hardness. If the treatment temperature crosses beyond the peak temperature, it is perhaps too high above the A_3 temperature of the alloy and austenite phase becomes stabilized again. This is substantiated by the optical micrographs. The attainment of peak hardness can be attributed to the following factors:

- i) Initially when the alloy is held just above the A_3 temperature, the solid solubility of carbon and other alloying elements being the lowest possible, the austenite matrix

gets depleted of carbon and other alloying elements with consequent fine alloy carbide precipitation.

- ii) The martensite start temperature (M_s) of the alloy depleted austenite matrix is raised and during subsequent air cooling the matrix transforms to martensite embedded with fine carbides.
- iii) On further increase in temperature, the austenite gets stabilized again because of the higher solid solubility and the precipitates are also coarsened resulting in a drop in hardness.

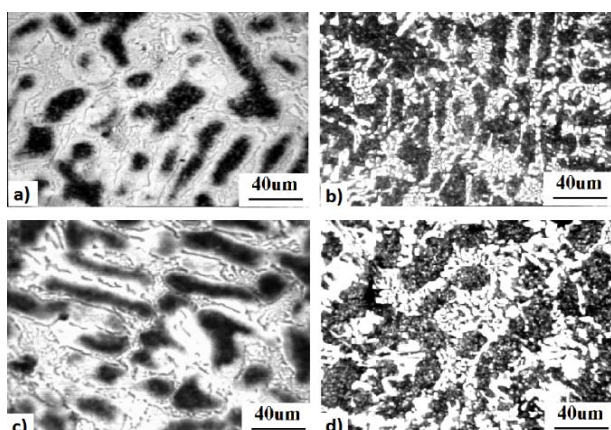


Fig. 6. Optical micrographs of isothermally treated Cr-Mn-Cu alloy for a) 3 hours and air cooled; b) 9 hours and air cooled; c) 3 hours and cryotreated and d) 9 hours and cryotreated.

The bulk hardness versus isothermal treatment time plot at the optimum temperature 1023K (750 °C) obtained from isochronal treatment is shown in Fig. 5. It is evident from the figure that the hardness initially increasing almost linearly with time and becomes steady at the latter stage of treatment. A gradual conversion of austenitic matrix into a dark matrix embedded with very fine alloy carbides are revealed in the corresponding optical micrographs (Fig. 6). The actual phase present in the matrix is difficult to be resolved under optical microscope. The as-cast supersaturated austenite matrix tends to attain equilibrium carbon and alloy contents with consequent rejection of these elements and on subsequent cooling to room temperature the alloy depleted austenite transforms to the dark phase. The dark matrix could be resolved under scanning electron microscope and it is found to be mostly fine bainite with few areas of martensite embedded with fine alloy carbides. The SEM image of the destabilized matrix is

shown in Fig. 7 and the EDS spectra obtained from secondary carbides is shown in Fig. 7a.

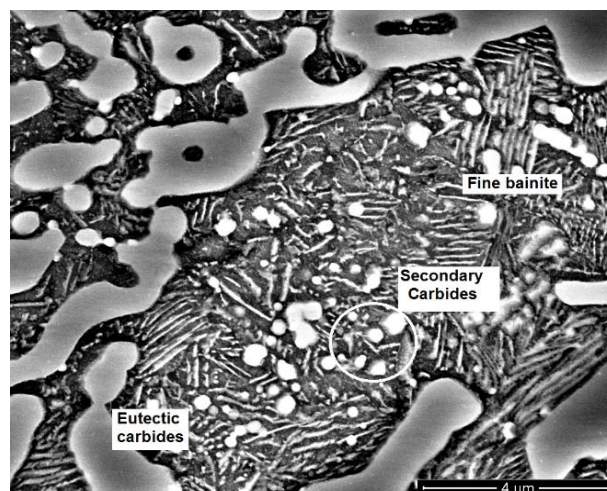


Fig. 7. SEM image of destabilized {1023K (750 °C) for 9 hours} and air cooled Cr-Mn-Cu alloy.

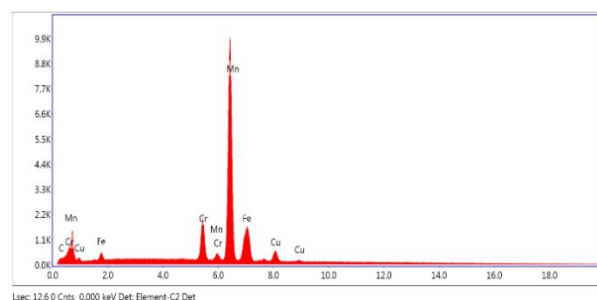


Fig. 7a. EDS spectra of secondary carbides in destabilized and air cooled alloy.

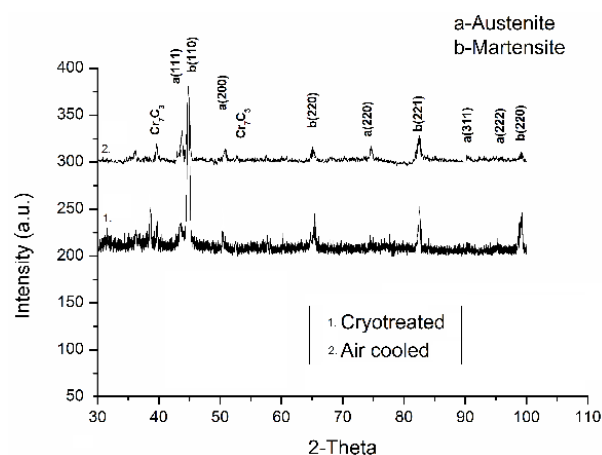


Fig. 8. XRD profile of i) destabilized and cryotreated alloy and ii) destabilized and air cooled alloy.

The effect of cryotreatment following isothermal destabilization for varying soaking periods on the bulk hardness is shown in Fig. 5. It depicts a similar trend as in the case of air cooling. However, in case of cryotreatment, the hardness increase is significantly higher than that in air

cooling. This trend can be justified with the retained austenite percentage measured from XRD analysis (Fig. 8) and the corresponding optical and SEM micrographs in Figs. 6 and 9 respectively. The EDS spectra from secondary carbides is shown in Fig. 9a.

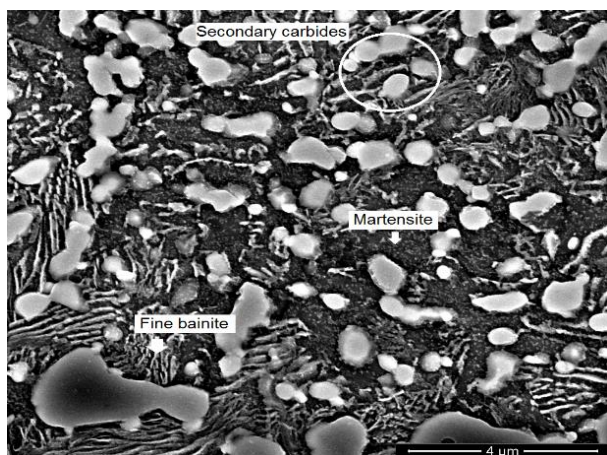


Fig. 9. SEM image of destabilized {1023K (750 °C) for 9 hours} and cryotreated Cr-Mn-Cu alloy.

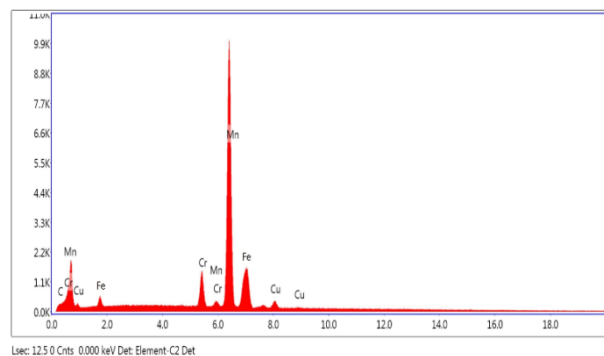


Fig. 9a. EDS spectra of secondary carbides formed in destabilized and cryotreated alloy.

Table 3. Details of carbide volume% and retained austenite content in different conditions.

Alloy conditions	Carbide volume%	Retained austenite%
1. As-cast	15.44	87.63
2. Destabilized at 1023K (750 °C) + 9 hrs. → air cooling	21.50	13.54
3. Destabilized at 1023K (750 °C) + 9 hrs. → cryotreatment	28.32	-

A large dispersion of very fine secondary carbide precipitates accounts for further increase in hardness which has been confirmed by the volume fraction of carbides determined by electrolytic extraction (Table 3). The matrix also contributes to the high hardness, a predominantly martensitic matrix with lesser

areas of fine bainites are formed as evidenced by the SEM.

3.2 Static corrosion rates

The static corrosion rates of destabilized and subsequently air cooled or cryotreated Cr-Mn-Cu and high chromium alloys in tap water (pH =7) are shown in Fig. 10. It is evident from the figure that cryotreated alloys are having a lower rate of corrosion than those of destabilized and air cooled alloys.

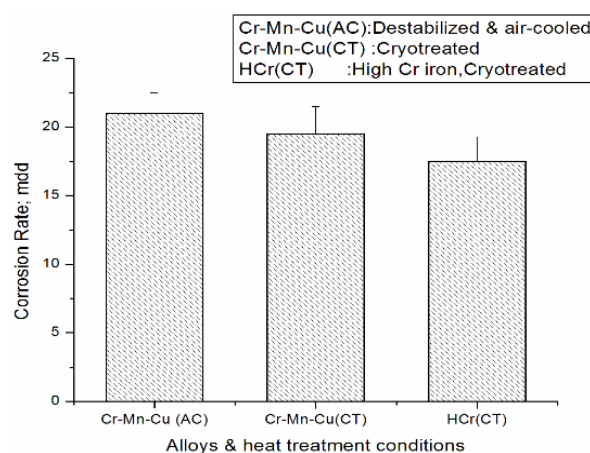


Fig. 10. Static aqueous corrosion rate in different alloy conditions.

Similar improvement in corrosion resistance has been observed by Amini K. et al. in cryotreated tool steel [30]. The improvement in corrosion resistance has been attributed to the more uniform carbide distribution in association with higher fine carbide formation in cryotreated alloy. It is believed that, the deep cryogenic treatment reduces the internal stress and stabilizes the dislocation structure in steel, consequently, decreasing the free energy of atoms. This results in a better corrosion resistance in steel [37,38].

3.3 Slurry-erosion behaviour

The cumulative wear loss versus wearing time curves are shown in Fig. 11, from which it is apparent that, the wear resistance of the cryotreated specimens is significantly improved compared to those in destabilized and subsequently air cooled specimens. The wear resistance of the as-cast alloy is least among other tested alloys. The erosive wear resistance of the cryotreated Cr-Mn-Cu alloys is comparable to that of cryotreated high

chromium alloy irons. The hardness perhaps plays a vital role in decreasing the wear rate. The corresponding microstructures obviously have a great influence on the wear loss. A fine Grained predominantly martensitic matrix with least amount of retained austenite embedded with fine and hard alloy carbides exhibit very good wear resistance. The better wear resistance of cryotreated samples can be attributed to three factors:

- I. Due to reduction of retained austenite and its conversion to higher percentage of martensite in the matrix. This provides stronger support to the hard and fine secondary alloy carbides during erosion.
- II. More homogeneous precipitation with high volume fraction of finer alloy carbides.
- III. Cryotreatment produces refined martensitic matrix causing a fine grained strengthening effect which improves wear resistance further.

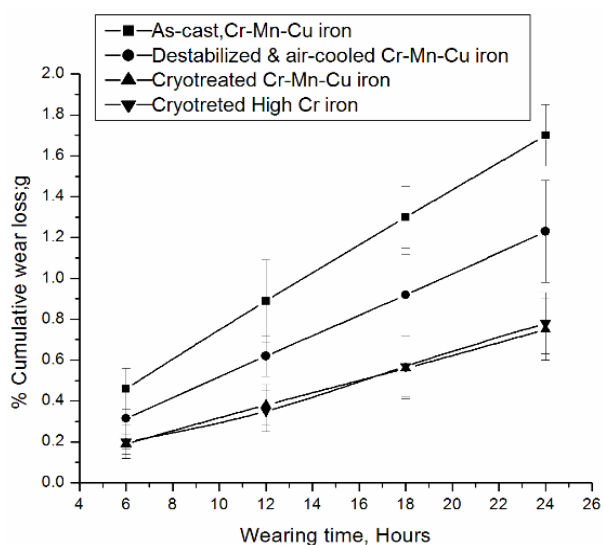


Fig. 11. Average cumulative wear loss vs. time plot in slurry erosion test.

The worn out surface topography have been studied with scanning electron microscope (SEM). The SEM micrographs show formation of indentation craters by ploughing mechanism as suggested by Hutchings [39]. The round to sub-angular shaped eroding particles impinges on the metal surface pushing the metal in the direction of the movement of the eroding particles. The erosion occurs due to fracture and detachment of this lip. The metal is displaced also at the sides of the impact craters. The worn out surface show the carbides in relief, being

harder phase compared to the matrix. The matrix regions have worn out preferentially leaving the carbide regions to support the load of eroding particles. In all the worn out surfaces plough marks are prominent in the matrix phases (Figs. 12a and 12b).

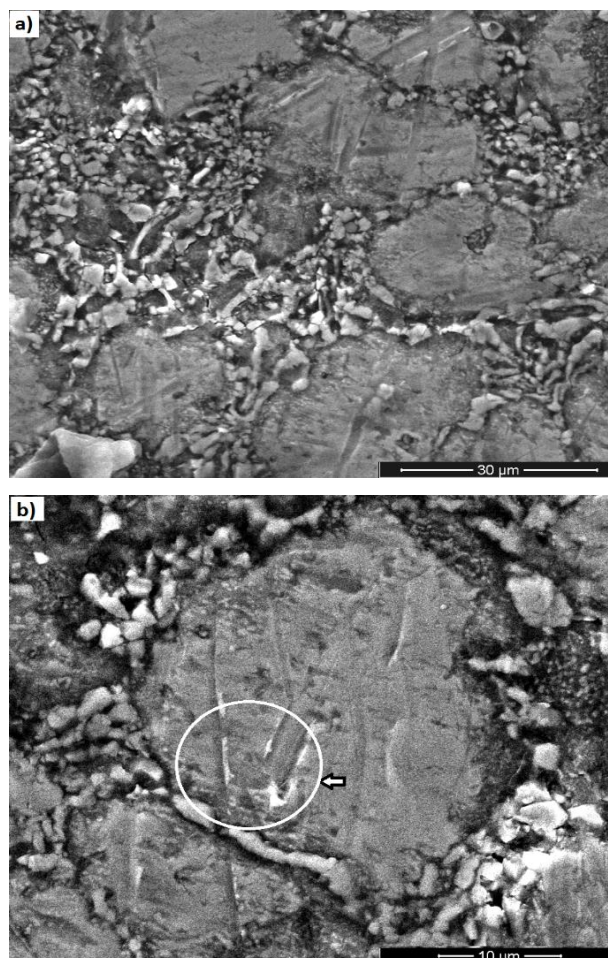


Fig. 12. a) SEM image of worn out surface of destabilized and air cooled alloy, b) Magnified image showing plough mark sand lip formation in the matrix.

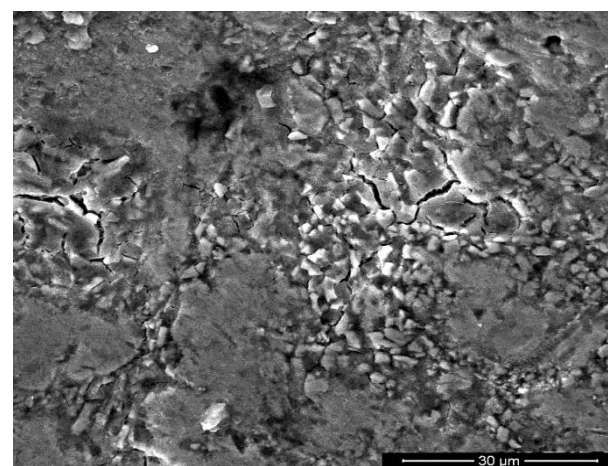


Fig. 13. SEM image of worn out surface of as- cast alloy showing micro-cracks in the matrix.

The as-cast Cr-Mn-Cu alloy shows fine cracks formed in the matrix. These cracks might have led to spall formation and hence material detachment (Fig. 13).

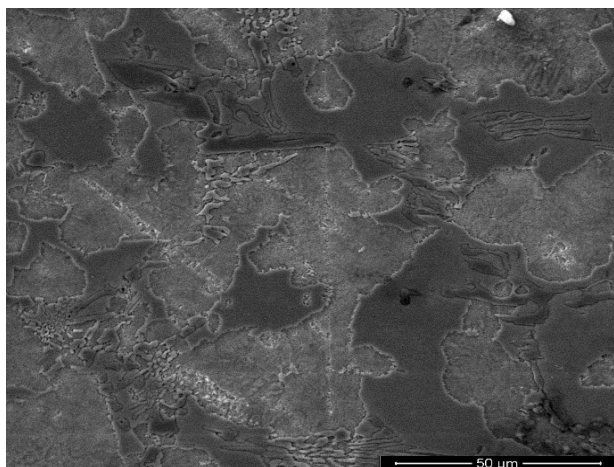


Fig. 14. SEM image of worn out surface of destabilized and cryotreated alloy showing smoother surface.

It was perhaps due to excessive preferential wear of the matrix regions for which carbides might become unsupported and susceptible to spalling and fracture. In contrast, cryotreated sample surfaces are smoother which can be attributed to their higher hardness resulting in shallow penetration and improved aqueous corrosion resistance hence lesser attack by corrosion- erosion (Fig. 14).

4. CONCLUSIONS

The Cr-Mn-Cu alloy iron consists of a predominantly austenitic matrix in as-cast condition. This as-cast matrix can be transformed to a hard martensitic and/or fine bainitic matrix embedded with fine M7C3 type secondary carbides by a destabilization treatment, conventionally employed for most wear resistance applications.

The retained austenite content in as-cast matrix cannot be fully eliminated by conventional destabilization treatment which can be almost totally converted to martensite by a destabilization followed by cryogenic treatment. The consequent bulk hardness increases significantly.

The slurry erosion resistance of the cryotreated Cr-Mn-Cu iron is well comparable to that of

cryotreated high chromium iron. Not only higher hardness but improved corrosion resistance contributes to better slurry erosion property.

It is evident from the SEM images of the worn out surfaces that, the predominant mechanism of material removal during slurry erosion is by ploughing. In as-cast irons cracks are formed around the matrix leading to spall formation. In case of cryotreated iron matrix being harder, no preferential erosion between matrix and carbides are occurring and hence a smoother worn out surface is revealed.

REFERENCES

- [1] J.T.H. Pearce, 'High chromium cast irons to resist abrasive wear', *Foundryman*, vol. 95, pp. 156-166, 2002.
- [2] C.P. Tabrett, I.R. Sare and M.R. Ghomashchi, 'Microstructure-property relationships in high chromium white iron alloys', *Int. Mater. Rev.*, vol. 41, no. 2, pp. 59-82, 1996.
- [3] J. Liu and Y. Man, 'Development of abrasive resistant Ni-hard 4 cast irons', *Wear*, vol. 162-164, pp. 833-836, 1993.
- [4] M. Salasi, G.B. Stachowiak and G.W. Stachowiak, 'Three-body tribocorrosion of high -chromium cast irons in neutral and alkaline environments', *Wear*, vol. 271, pp. 1385-1396, 2011.
- [5] G.B. Stachowiak, G.W. Stachowiak and O. Celliers, 'Ball-cratering abrasion tests of high-Cr white cast irons', *Tribol Int.*, vol. 38, pp. 1076-1087, 2005.
- [6] E. Zumelzu, L. Goyos, C. Cabezas, O. Opitz and A. Parada, 'Wear and corrosion behaviour of high-chromium (14-30% Cr) cast iron alloys', *J. Mater. Process. Tech.*, vol. 128, pp. 250-255, 2008.
- [7] J.O. Agunsoye and A.A. Ayeni, 'Effect of Heat Treatment on the Abrasive Wear Behavior of High Chromium Iron under Dry Sliding Condition', *Tribology in Industry*, vol. 34, no. 2, pp. 82-91, 2012.
- [8] J.F. Flores, A. Neville, N. Kapur and A. Gnanavelu, 'Erosion-corrosion degradation mechanisms of Fe-Cr-C and WC-Fe-Cr-C PTA overlays in concentrated slurries', *Wear*, vol. 267, no. 11, pp. 1811-1820, 2009.
- [9] H.H. Tian, G.R. Addie and R.J. Visintainer, 'Erosion-corrosion performance of high-Cr cast iron alloys in flowing liquid-solid slurries', *Wear*, vol. 267, no. 11, pp. 2039-2047, 2009.

- [10] L.I. Levi et al., 'Wear resistant chromium-manganese cast irons', *Russ. Cast. Prod.*, August, pp. 409-412, 1967.
- [11] A. Basak, J. Penning and J. Dilewijns, 'Effect of Mn on wear resistance and impact strength of 12% Cr white cast irons', *Int. Cast Met. J.*, vol. 6, no. 3, pp. 12-17, 1981.
- [12] A. Basak, J. Penning and J. Dilewijns, 'Effect of Ti inoculation on wear resistance and impact strength of Cr-Mn alloy white cast irons', *Met. Technol.*, vol. 9, no. 9, pp. 381-384, 1982.
- [13] I. Chakrabarty and A. Basak, 'Ausaging and corrosive wear behavior of Cr-Mn-Cu white cast irons', *AFS Trans.*, vol. 98, pp. 707-716, 1990.
- [14] I. Chakrabarty, A. Basak and U.K. Chatterjee, 'Corrosive wear behavior of Cr-Mn-Cu white cast irons in sand-water slurry media', *Wear*, vol. 143, pp. 203-220, 1991.
- [15] I. Chakrabarty, 'Effect of copper on the corrosion resistance behavior of as-cast and destabilized Cr-Mn white cast irons', *AFS Int. J. Metal Cast.*, vol. 5, no. 1, pp. 49-56, 2011.
- [16] P.N.V.R.S.S.V Prasada Rao, A.K. Patwardhan and N.C. Jain, 'Effect of microstructure on the corrosion and deformation behavior of a newly developed 6Mn-5Cr-1.5Cu corrosion-resistant white iron', *Metall. Mater. Trans. A*, vol. 24, no. 2, pp. 445-457, 1993.
- [17] A.K. Patwardhan and N.C. Jain, 'Modeling of the corrosion behavior and its interrelation with the deformation behavior and microstructure in a newly developed 7.5Mn-5Cr-1.5Cu alloy white iron', *Metall. Mater. Trans. A*, vol. 22, no. 10, pp. 2319-2325, 1991.
- [18] D. Das, A.K Dutta, V. Toppo and K.K. Ray, 'Effect of deep cryogenic treatment on the carbide precipitation and tribological behavior of D2 steel', *Materials and Manufacturing Processes*, vol. 22, pp. 474-480, 2007.
- [19] D. Das, R. Sarkar, A.K Dutta and K.K. Ray, 'Influence of sub-zero treatments on fracture toughness of AISI D2 steel', *Mater. Sci. Eng. A*, vol. 528, pp. 589-603, 2010.
- [20] A.J. Vimal, A. Bensely, D. Mohan Lal and K. Srinivasan, 'Deep cryogenic treatment improves wear resistance of En 31 steel', *Materials and Manufacturing Processes*, vol. 23, no. 4, pp. 369-376, 2008.
- [21] N.S. Kalsi, R. Sehgal and V.S. Sharma, 'Cryogenic treatment of tool materials: A Review', *Materials and Manufacturing Processes*, vol. 25, no. 10, pp. 1077-1100, 2010.
- [22] M.A. Jaswin and D. Mohan Lal, 'Optimization of the cryogenic treatment process for En 52 valve steel using Grey-Taguchi method', *Materials and Manufacturing Processes*, vol. 25, no. 8, pp. 842-850, 2010.
- [23] M. Koneshlou, K.M. Asl and F. Khomamizadeh, 'Effect of cryogenic treatment on microstructure, mechanical and wear behaviors of AISI H13 hot work tool steel', *Cryogenics*, vol. 51, pp. 55-61, 2011.
- [24] K Amini, S. Nategh and A. Shafyei, 'Influence of different cryotreatments on tribological behavior of 80Cr Mo12 5 cold work tool steel', *Mater. Des.*, vol. 31, pp. 4666-4675, 2010.
- [25] D. Senthilkumar and I. Rajendran, 'Optimization of deep cryogenic treatment to reduce wear loss of 4140 steel', *Materials and Manufacturing Processes*, vol. 27, pp. 567-572, 2012.
- [26] M. El Mehtedi, P. Ricci, L. Drudi, S. El Mohtadi, M. Cabibbo and S. Spigarelli, 'Analysis of the effect of deep cryogenic treatment on the hardness and microstructure of X30 Cr Mo N15 1 steel', *Mater. Des.*, vol. 33, pp. 136-144, 2012.
- [27] R. Sri Siva, A. Arockia Jaswin and D. Mohan Lal, 'Enhancing the wear resistance of 100 Cr6 bearing steel using cryogenic treatment', *Tribology Transactions*, vol. 55, pp. 387- 393, 2012.
- [28] M. Arockia Jaswin and D. Mohan Lal, 'Effect of cryogenic treatment on the tensile behavior of En 52 and 21-4N valve steels at room and elevated temperature', *Mater. Des.*, vol. 32, pp. 2429-2437, 2011.
- [29] P. Baldissera, 'Deep cryogenic treatment of AISI 302 stainless steel: Part I- hardness and tensile properties', *Mater. Des.*, vol. 31, pp. 4725-4730, 2010.
- [30] K. Amini, A. Akhbarizadeh and S. Javadpour, 'Investigating the effect of the quench environment on the final microstructure and wear behavior of 1.2080 tool steel after deep cryogenic heat treatment', *Mater. Des.*, vol. 45, pp. 316-322, 2013.
- [31] Shaohong Li, Na Min, Junwan Li, Xiaochun Wu, Chenhui Li and Leilei Tang, 'Experimental verification of segregation of carbon and precipitation of carbides due to deep cryogenic treatment for tool steel by internal friction method', *Mater. Sci. Eng. A*, vol. 575, pp. 51-60, 2013.
- [32] V.G. Gavriljuk, W. Theisen, V.V. Sirosh, E.V. Polsin, A.Kortmann, G.S. Mogilny, Yu.N. Petrov and Ye. V. Tarusin, 'Low temperature martensitic transformation in tool steels in

- relation to their deep cryogenic treatment', *Acta Mater.*, vol. 61, pp. 1705-1715, 2013.
- [33] Hong- Shan Yang, Jun Wang, Bao-Luo Shan, Hao-huai Liu, Sheng-Ji Gao and Si-Jiu Huang, 'Effect of cryogenic treatment on the matrix structure and abrasion resistance of white cast iron subjected to destabilization treatment', *Wear*, vol. 261, pp. 1150-1154, 2006.
- [34] Hao-huai Liu, Jun Wang, Bao-Luo Shan, Hong-Shan Yang, Sheng-Ji Gao and Si-Jiu Huang, 'Effects of deep cryogenic treatment on property of 3Cr13Mo1V1.5 high chromium cast iron', *Mater. Des.*, vol. 28, pp. 1059-1064, 2007.
- [35] Hao-Huai Liu et al., 'Effects of cryogenic treatment on microstructure and abrasion resistance of CrMnB high- chromium iron subjected to sub-critical treatment', *Mater Sci. Eng. A*, vol. 478, pp. 324-328, 2008.
- [36] C.P. Tabrett and I.R. Sare, 'Effect of high temperature and sub-ambient treatments on the matrix structure and abrasion resistance of a high chromium white iron', *Scripta Mater.*, vol. 38, no. 12, pp. 1747-1753, 1998.
- [37] R.F. Barron and R.H. Thompson, 'Effects of cryogenic treatment on corrosion resistance', [Paper BP-17] in Fast RW (Ed.), International cryogenic materials conference, New York; Plenum Press, 1989.
- [38] Xuan Fu-Zhen, Huang, Xiaoqing and Tu, Shan-Tung, 'Comparison of 30Cr2Ni4MoV rotor steel with treatments on corrosion resistance in high temperature water', *Mater. Des.*, vol. 29, pp. 1533, 2008.
- [39] I.M. Hutchings, *Tribology - Friction and Wear of Engineering Materials*, Edward Arnold, 1992.